



Applied Mathematics and Nonlinear Sciences

<https://www.sciendo.com>

Monotonicity and non-monotonicity regions of topological entropy for Lorenz-like families with infinite derivatives

M.I. Malkin^{1,2}, K.A. Safonov^{1,2} [†]

¹Lobachevsky State University of Nizhniy Novgorod, Russia

²National Research University Higher School of Economics, Russia

Submission Info

Communicated by Lyudmila Sergeevna Efremova

Received January 8th 2020

Accepted April 11th 2020

Available online November 16th 2020

Abstract

We study behavior of the topological entropy as the function of parameters for two-parameter family of symmetric Lorenz maps $T_{c,\varepsilon}(x) = (-1 + c|x|^{1-\varepsilon}) \cdot \text{sgn}(x)$. This is the normal form for splitting the homoclinic loop in systems which have a saddle equilibrium with one-dimensional unstable manifold and zero saddle value. Due to L.P. Shilnikov results, such a bifurcation corresponds to the birth of Lorenz attractor (when the saddle value becomes positive). We indicate those regions in the bifurcation plane where the topological entropy depends monotonically on the parameter c , as well as those for which the monotonicity does not take place. Also, we indicate the corresponding bifurcations for the Lorenz attractors.

Keywords: topological entropy, Lorenz attractor, homoclinic bifurcation, jump of entropy

AMS 2010 codes: 37B40, 37D45, 37G20

1 Introduction

The paper is devoted to the study of one-dimensional factor map for the geometric model of Lorenz attractors in the form of two-parameter family of Lorenz maps on the interval $I = [-1, 1]$ given by

$$T_{c,\varepsilon}(x) = (-1 + c \cdot |x|^{1-\varepsilon}) \cdot \text{sgn}(x) \quad (1)$$

Here the parameters c, ε satisfy the inequalities

1. $0 < c \leq 2$, which guarantees the invariance of the interval I ;
2. $0 < \varepsilon < 1$, which corresponds to positive saddle value in the geometric Lorenz model (see below) and implies infinite one-sided derivatives at the discontinuity point.

[†]Corresponding author.

Email address: safonov.klim@yandex.ru

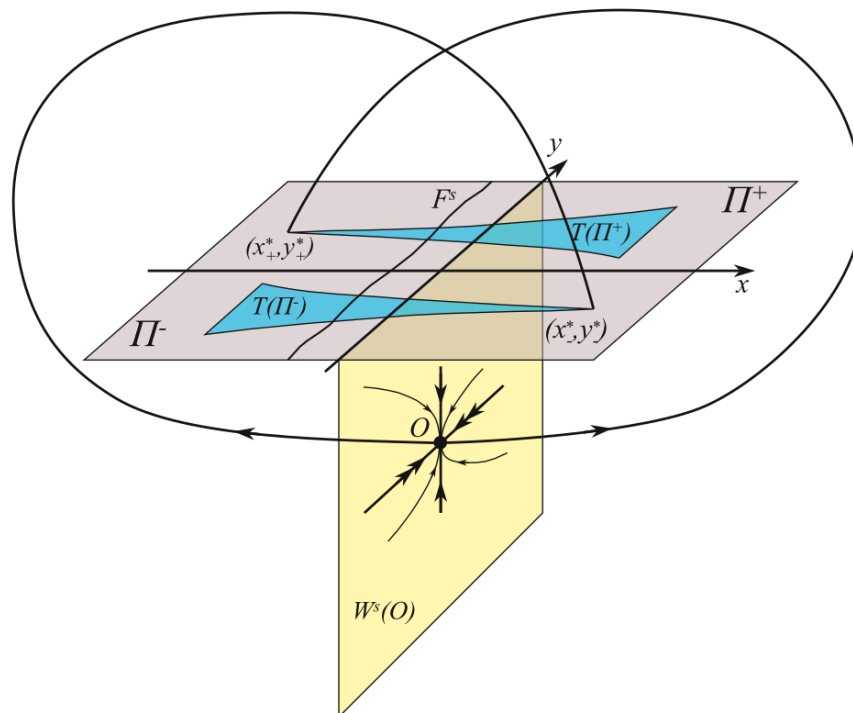


Fig. 1 Afraimovich-Bykov-Shilnikov geometric model of Lorenz attractor

Such families of maps appear naturally in the studies of bifurcations related to the birth of Lorenz attractor from the separatrix loop with zero saddle value. Based on the geometric model of Lorenz attractor by Afraimovich, Bykov and Shilnikov [1], consider a system of $(n + 1)$ differential equations with the saddle O having one-dimensional unstable manifold for the eigenvalue $\gamma > 0$; we also assume that among other eigenvalues, the smallest one (with respect to the absolute value), say λ_1 , is real, so that we have $\operatorname{Re} \lambda_i < \lambda_1 < 0$ ($i = 2, \dots, n$). The next assumption is the following: there is a section D which is transverse to the stable manifold $W^s(O)$ and invariant under the Poincaré map $T : D \rightarrow D$. If one introduces the coordinates (\mathbf{x}, y) on D such that the line $y = 0$ corresponds to the trace of the stable manifold $D \cap W^s(O)$, the map T can be written as

$$f_{\pm}(\mathbf{x}, y) = \mathbf{x}_{\pm}^* + B_{\pm}|y|^v + \phi_{\pm}(\mathbf{x}, y),$$

$$g_{\pm}(\mathbf{x}, y) = y_{\pm}^* + A_{\pm}|y|^v + \psi_{\pm}(\mathbf{x}, y),$$

where $v = -\frac{\gamma}{\lambda_1} < 1$ is the saddle index of O and (\mathbf{x}_+, y_+) , (\mathbf{x}_-, y_-) are the points of intersection of unstable manifolds with D (see the cusps in fig. 1); A_{\pm} , B_{\pm} are nonzero coefficients and $\phi_{\pm}(\mathbf{x}, y)$, $\psi_{\pm}(\mathbf{x}, y)$ are smaller remainder terms.

The main conditions in the above geometric model are the hyperbolic ones for the section D : namely, the following is supposed to hold

$$\begin{aligned} & a) \left\| \frac{\partial f_{\pm}}{\partial \mathbf{x}} \right\| < 1, \quad b) \left\| \left(\frac{\partial g_{\pm}}{\partial y} \right)^{-1} \right\| < 1, \\ & c) 1 - \left\| \frac{\partial f_{\pm}}{\partial \mathbf{x}} \right\| \cdot \left\| \left(\frac{\partial g_{\pm}}{\partial y} \right)^{-1} \right\| > 2 \cdot \sqrt{\left\| \left(\frac{\partial g_{\pm}}{\partial y} \right)^{-1} \cdot \frac{\partial f_{\pm}}{\partial y} \right\| \cdot \left\| \left(\frac{\partial g_{\pm}}{\partial y} \right)^{-1} \right\| \cdot \left\| \frac{\partial g_{\pm}}{\partial \mathbf{x}} \right\|}, \\ & d) \left\| \left(\frac{\partial g_{\pm}}{\partial y} \right)^{-1} \cdot \frac{\partial f_{\pm}}{\partial y} \right\| \cdot \left\| \frac{\partial g_{\pm}}{\partial \mathbf{x}} \right\| < (1 - \left\| \frac{\partial f_{\pm}}{\partial \mathbf{x}} \right\|)(1 - \left\| \left(\frac{\partial g_{\pm}}{\partial y} \right)^{-1} \right\|). \end{aligned} \quad (2)$$

These conditions imply the existence of invariant stable foliation on D whose leaves are Lipschitz of the form $y = h(x)$. The factor map $\tilde{T}(y)$ for the Poincaré map along the leaves $y = h(x)$ of the stable foliation

is a one-dimensional map with the single discontinuity point $y = 0$ and two monotonicity intervals for $y > 0$ and $y < 0$. The factor one-dimensional map is usually called the Lorenz map (or Lorenz-like map). More precisely, it is an interval map with one discontinuity point and two continuous, monotone increasing branches. By appropriate scaling one may assume that the interval is $[-1, 1]$, the discontinuity point is 0, and

$$\lim_{x \rightarrow 0+} T(x) = T(0+) = -1, \quad \lim_{x \rightarrow 0-} T(x) = T(0-) = 1^a$$

Symmetry of Lorenz map (like in the original Lorenz equation and in the family under consideration) means that $T(x) = -T(-x)$.

One of the criteria for the birth of Lorenz attractor (see [2, 3]) is the presence of the homoclinic butterfly to the equilibrium state with zero saddle value. In more details, assume that the unstable separatrices Γ_1 and Γ_2 of the saddle O tend to O as $t \rightarrow \infty$, so that they are tangent to the leading stable direction (which corresponds to the eigenvalue λ_1) touching it from the same side with respect to the strong stable manifold, and the following equality holds; $\gamma + \lambda_1 = 0$. This bifurcation is related to the Poincaré map of the form

$$\begin{aligned} f_{\pm}(\mathbf{x}, y) &= \mathbf{x}_{\pm}^* + B_{\pm}|y|^{1-\varepsilon} + \phi_{\pm}(\mathbf{x}, y, \mu_{\pm}, \varepsilon), \\ g_{\pm}(\mathbf{x}, y) &= \mu_{\pm} + A_{\pm}|y|^{1-\varepsilon} + \psi_{\pm}(\mathbf{x}, y, \mu_{\pm}, \varepsilon). \end{aligned} \quad (3)$$

The above assumptions imply the following result on the birth of Lorenz attractors.

Theorem 1. (Shilnikov, [2]) *If $0 < |A_{\pm}| < 2$ for the map (3), then in the parameter plane (μ, ε) there is a region V_{LA} such that $(0, 0)$ belongs to the closure $\overline{V_{LA}}$, and for every point $(\mu, \varepsilon) \in V_{LA}$, the initial flow has Lorenz attractor.*

Consider a system of differential equations which admits some involution R . Moreover, assume that the equilibrium state O satisfies $R(O) = O$. Then, according to the Bochner-Montgomery theorem, one may consider that the involution acts linearly in a neighborhood of O . Denote by e_0 and e_1 the eigenvectors corresponding to the eigenvalues γ and λ_1 , respectively, and assume that $R(e_0) = -e_0$ and $R(e_1) = e_1$. In this case, in the space of dynamical systems having the symmetries with the above properties, the bifurcation described in Theorem 1 belongs to a codimension-2 bifurcation set, and thus, it may appear in two-parameter families of differential equations. In particular, the well-known Shimizu-Morioka equations provide an example of such a system:

$$\begin{cases} \dot{x} = y, \\ \dot{y} = x \cdot (1 - z) - \lambda y, \\ \dot{z} = -\alpha \cdot z + x^2. \end{cases} \quad (4)$$

In [4], the system (4) is shown to appear as the normal form in studying the local bifurcations of the equilibrium state which has zero eigenvalue with multiplicity 3. Also the parameter values corresponding to the existence of the Lorenz attractor in this system have been found numerically. Later, A. Shilnikov studied the Shimizu-Morioka system in more details ([5, 6]). Note that in [6] the kneading technique was applied for studying the system (4) (see the section 3 below for definitions and some results of the kneading theory). In particular, one of the results of those studies is the following fact: in the parameter plane (α, λ) , the boundary of the region corresponding to the existence of Lorenz attractor, contains the system having homoclinic figure-8 loop at a saddle with zero saddle value (see fig. 2). Presence of this bifurcation in the system (4) has been proven analytically in [7]; however, the problem on finding the estimate on the separatrix value A , which would allow to apply theorem 1, remained open, until recently it was obtained in [8] that $0.625 < A < 0.627$ (using the computer assisted proof).

^a The latter conditions could be assumed without loss of generality because outside the interval $[T(0+), T(0-)]$ each point is wandering and dynamics is trivial.

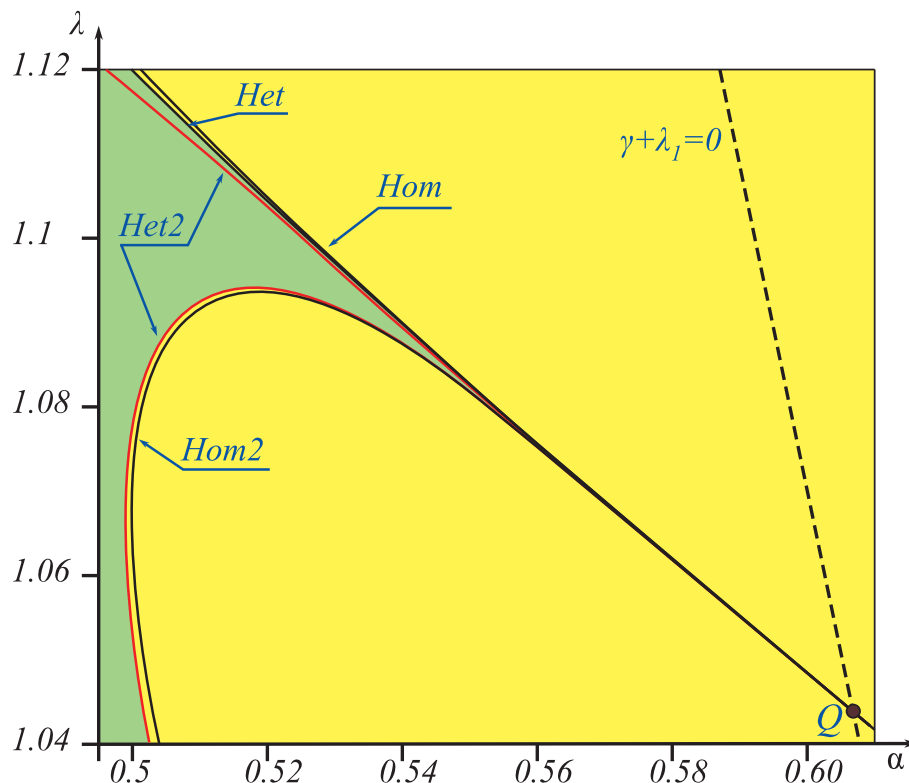


Fig. 2 Bifurcation diagram for the Shimizu-Morioka system near the point $Q(\alpha = 0.608, \lambda = 1.044)$ which corresponds to the homoclinic figure-8 bifurcation to a saddle with zero saddle value. (The green region corresponds to parameter values where the Lorenz attractor exists.)

Further we will assume that the system under consideration possesses symmetry and that $A_{\pm} > 0$. In this case the region where attractor V_{LA} exists, lies in the half-plane $\mu < 0$, and the factor map with respect to the stable foliation is of the form

$$\bar{y} = (-\mu + A|y|^{1-\varepsilon} + o(|y|^{1-\varepsilon})) \cdot \text{sgn}(y).$$

Consider the truncated factor map obtained by omitting small terms

$$\bar{y} = (-\mu + A|y|^{1-\varepsilon}) \cdot \text{sgn}(y).$$

Denoting the coordinate $y = \mu x$ ($\mu > 0$) we get the formula for the map under consideration in the present paper

$$\begin{aligned} \mu \bar{x} &= (-\mu + A\mu^{1-\varepsilon}|x|^{1-\varepsilon}) \cdot \text{sgn}(x), \\ \bar{x} &= (-1 + c|x|^{1-\varepsilon}) \cdot \text{sgn}(x), \text{ where } c = A\mu^{-\varepsilon}. \end{aligned}$$

Note that this change of coordinates is degenerate at $\mu = 0$ and so, the line $\mu = 0$ in the parameter plane (μ, ε) , which corresponds to systems with homoclinic loops, is transformed to $c = \infty$ in the parameter plane (c, ε) . Since the value $\mu^{-\varepsilon}$ can attain any number from 1 to ∞ as $c, \varepsilon \rightarrow 0$, it follows that the point $(\mu = 0, \varepsilon = 0)$, which corresponds to the homoclinic butterfly bifurcation of the saddle with zero saddle value in the initial system, is transformed into the whole straight line $\varepsilon = 0$. Therefore the map $T_{c,\varepsilon}$ with ε small is related to the bifurcation of birth of attractor from the separatrix loop with zero saddle value.

The paper is organised as follows. Section 2 contains the construction of bifurcation diagram in the parameter space (c, ε) . We indicate the bifurcation curves which divides the parameter plane into regions with different number of connected components of attractor and indicate some other dynamical features. We also add the lines of constant topological entropy (the kneading charts) to this diagram.

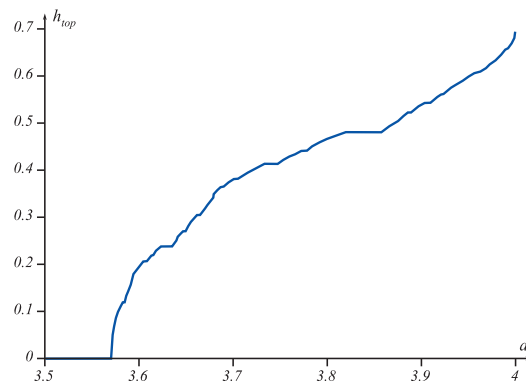


Fig. 3 The graph of topological entropy for the logistic map $f_a(x) = ax(1-x)$.

In Section 3 we consider the entropy and kneading aspects of dynamics of the family $T_{c,\varepsilon}$. We study the problems of continuity and monotonicity of topological entropy as the function of the parameter c . Note that the problems of monotonicity of topological entropy was considered for specific families of one dimensional maps by several authors. In [9], [10] it has been proven that for quadratic maps $x^2 + c$, the topological entropy is a monotone (non strictly) increasing function of c (see fig. 3 for the logistic family, which is actually the same after change of coordinates). In recent paper [11], the monotonicity result was proven for the family $x^\ell + c$ with ℓ large (not necessarily integer). Our family of maps is different from those families in the sense that we allow infinite derivatives at the discontinuity point, which makes the problem even more complicated because the complex analysis technique doesn't work here.

We show that for ε fixed, in the one-parameter family $T_c = T_{c,\varepsilon}$, the topological entropy is not monotone. We show numerically that the topological entropy as the function of c has a single minimum in certain region. Also we show that in the case when $T_{c,\varepsilon}$ is expanding ($DT \geq q > 1$), the topological entropy is monotone increasing in c .

2 Bifurcation diagram

In this section we study principal bifurcations of the map $T_{c,\varepsilon}$ in the region $1 \leq c \leq 2$, $0 \leq \varepsilon \leq 1$ of the parameter plane. Note that we consider the map $T_{c,\varepsilon}$ not only for ε small, and hence, some of our results lie beyond the applications in the geometric Lorenz model (in particular, the condition b) in (2) is satisfied not for all regions we consider here)

The figure 4 presents the bifurcation diagram. It makes sense to consider this diagram together with the chart of the kneading invariants presented in figure 5. The notion of the kneading invariant is discussed in details below in section 3. Now we only stress that under some natural assumptions (like expanding ones) the kneading invariant is the complete invariant of topological conjugation, and in more general case, the points with the same kneading invariant have similar orbits (up to so-called combinatorial equivalence). Thus, the kneading chart along with the bifurcation diagram allow to realize fairly complete picture of dynamical and topological structure.

Further we will describe the regions in the bifurcation diagram as well as the curves which partition these regions. First we explain the reason for considering the values c just from the interval $[1, 2]$.

The case when $c > 2$. If $c > 2$, the dynamical behavior is as follows. The interval I is no longer invariant under $T_{c,\varepsilon}$. Indeed, for such c two unstable fixed point $x'' > 0$ and $-x''$ belong to the interval I (see fig. 6) and any point from subintervals $(x'', 1)$ and $(-1, -x'')$ tends to the stable fixed points x^s or $-x^s$, respectively, outside the interval I (here we consider the map $T_{c,\varepsilon}$ on the whole real line; note that $T_{c,\varepsilon}$ is well defined on \mathbb{R} due to formula (1)). The same happens to every preimage of these two subintervals. The restriction of $T_{c,\varepsilon}$ to

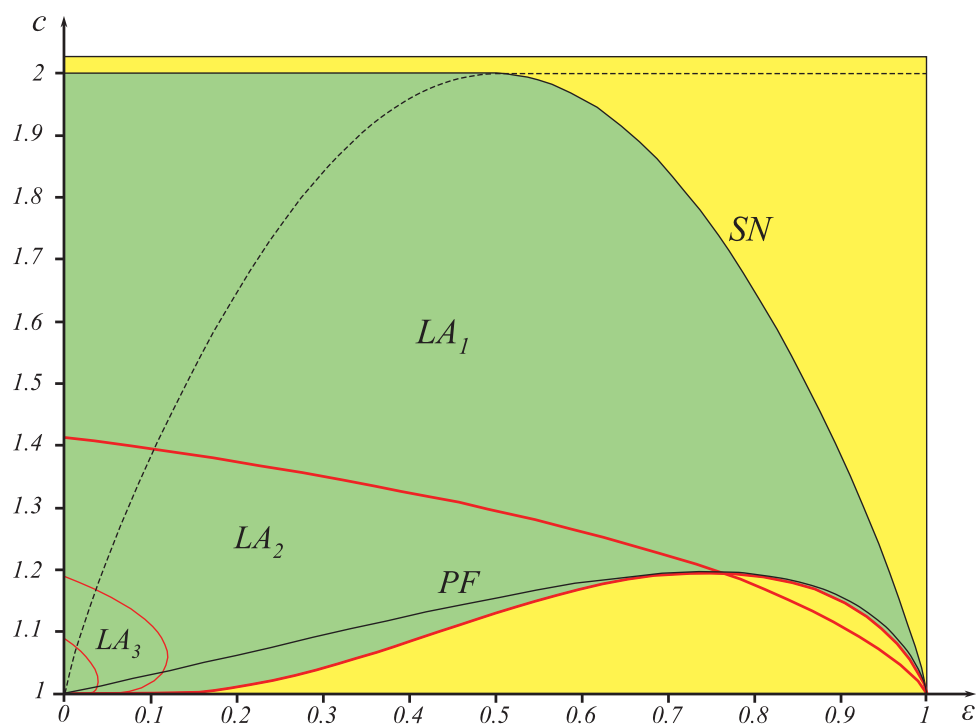


Fig. 4 The bifurcation diagram for map $T_{c,\epsilon}$. Green region correspond to the existence of Lorenz attractor.

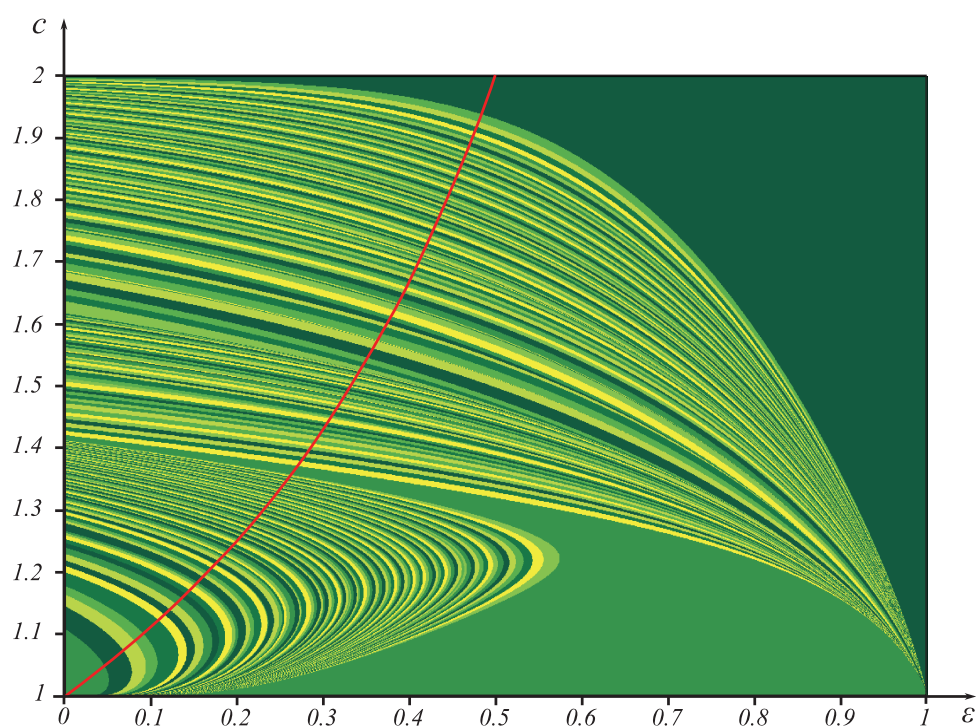


Fig. 5 The kneading chart for map $T_{c,\epsilon}$ shows that the topological entropy as the function of c has a single minimum for ϵ in the interval $[0, 0.6]$ (more precise calculation gives $\epsilon \in [0, 0.76]$). Above the red line one has that $T_{c,\epsilon}$ is expanding ($DT_{c,\epsilon} > 1$), and there the topological entropy is monotone increasing in c .

the interval $[-x'', x'']$ is an expanding map because, due to monotonicity of the derivative, one has the inequality $DT(x) \geq DT(x'') > 1$. So almost all points (with respect to Lebesgue measure) tend to the two stable fixed points. By standard arguments using the expanding condition, the nonwandering set $NW(T_{c,\varepsilon})$ consists of a Cantor set (the set of points not escaping from the interval I), and moreover, the map $T_{c,\varepsilon}$ restricted to this set is conjugate to the one-sided Bernoulli shift with two symbols.

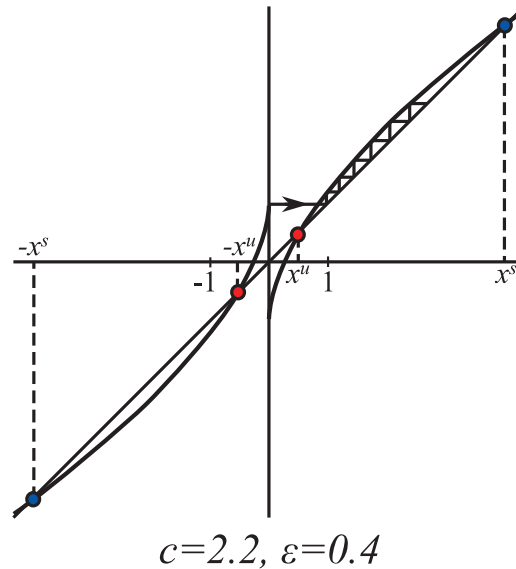


Fig. 6 The graph of $T_{c,\varepsilon}$ and the trajectory of the discontinuity point for $c > 2$.

The case when $0 < c < 1$. If $0 < c < 1$, the dynamics of $T_{c,\varepsilon}$ is trivial: all orbits converge to the stable periodic orbit of period two, which will be denoted by

$$(p^s, q^s), \text{ where } p^s < 0 < q^s.$$

It follows from uniqueness of stable period-2 orbit along with the symmetry of the map that

$$-1 + c \cdot x^{1-\varepsilon} = -x.$$

The case when $c = 1$. If $c = 1$ (see fig. 7), the point $x = 1$ is mapped into $T_{1,\varepsilon}(1) = 0$, i.e., the discontinuity point is of period 2. This bifurcation line $c = 1$ corresponds to the presence of a pair of two-round homoclinic loops in the three dimensional flow. The yellow region adjacent to the axis $c = 1$ in fig. 4 corresponds to the birth (from the discontinuity point) of two unstable period-2 points which will be denoted by (p_1'', q_1'') and (p_2'', q_2'') . We have

$$p_1'' < p^s < p_2'' < 0 < q_1'' < q^s < q_2'',$$

and the trajectory of the discontinuity point gets into the basin of the stable point. Since

$$T_{c,\varepsilon}^2[0, q_1''] = T_{c,\varepsilon}[-1, p_1''] \supset [p_2'', q_1''];$$

$$T_{c,\varepsilon}^2[p_2'', 0] = T_{c,\varepsilon}[q_2'', 1] \supset [p_2'', q_1''],$$

it follows (it is enough to apply the same arguments as in the case $c > 2$ for the second iteration $T_{c,\varepsilon}^2$) that the nonwandering set consists of a stable periodic orbit and a Cantor set, the dynamics on which is conjugate to the Bernoulli shift with two symbols.

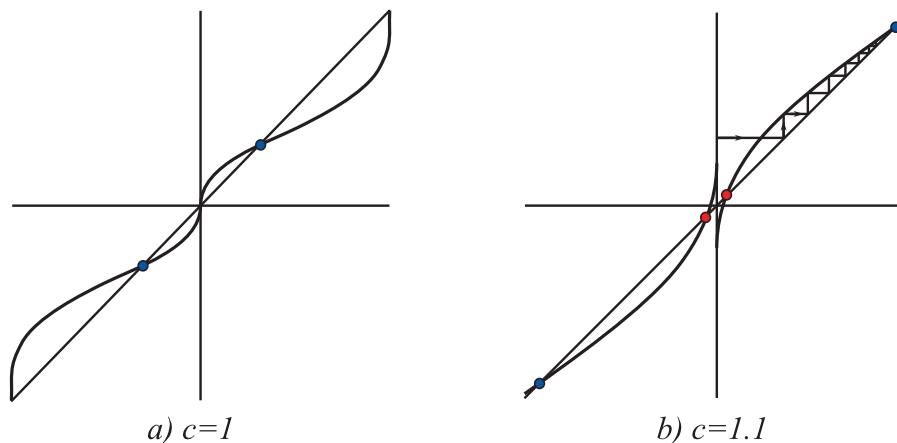


Fig. 7 The second iteration of the map $T_{c,\varepsilon}$ for $\varepsilon = 0.7$ with $c = 1$ (fig. a) and $c = 1.1$ (fig.b). In fig. b, a magnified fragment near the discontinuity point is shown.

Pitchfork bifurcation. The curve PF in fig. 4 corresponds to the fusion of three periodic orbits of period 2 (see the case above) into a single unstable orbit of period two. The equation of this curve can be obtained from

$$-1 + c \cdot x^{1-\varepsilon} = -x \quad (\text{period-2 condition}),$$

$$c(1 - \varepsilon) \cdot x^{-\varepsilon} = 1 \quad (\text{the tangency condition}),$$

here for the tangency condition we used the symmetry of period-2 orbit. So we get the equation for the bifurcation curve PF

$$c(1 - \varepsilon) \cdot \left(\frac{1 - \varepsilon}{2 - \varepsilon} \right)^{-\varepsilon} = 1 \quad (5)$$

Saddle-node bifurcation. In the upper yellow region (in $[0, 1] \times [1, 2]$) in fig. 4, the map acts similarly to the one for $c > 2$: namely, the nonwandering set consists of two stable fixed points and a Cantor set, so that the dynamics on this Cantor set is conjugate to the Bernoulli shift with two symbols. Other (wandering) points converge to the two stable fixed points. The boundary of this region is the saddle-node bifurcation curve, which is given by

$$-1 + c \cdot x^{1-\varepsilon} = x,$$

$$c(1 - \varepsilon) \cdot x^{-\varepsilon} = 1.$$

The fixed point at which this bifurcation takes place is the following

$$x = \frac{1 - \varepsilon}{\varepsilon}, \quad (6)$$

so the equation of the curve is of the form

$$c(1 - \varepsilon) \cdot \left(\frac{1 - \varepsilon}{\varepsilon} \right)^{-\varepsilon} = 1.$$

Note that the boundary of the yellow region is that part of the curve for which $x \leq 1$, i.e., $\varepsilon \geq \frac{1}{2}$ (see (6)).

The region where the attractor exists. In the green region in fig. 4 the map $T_{c,\varepsilon}$ has a nontrivial attractor (numerical evidence). By attractor A we mean a closed invariant set which has an absorbing open domain $U \supset A$ with

$$\overline{f(U)} \subset U, \quad A = \bigcap_n f^n(U).$$

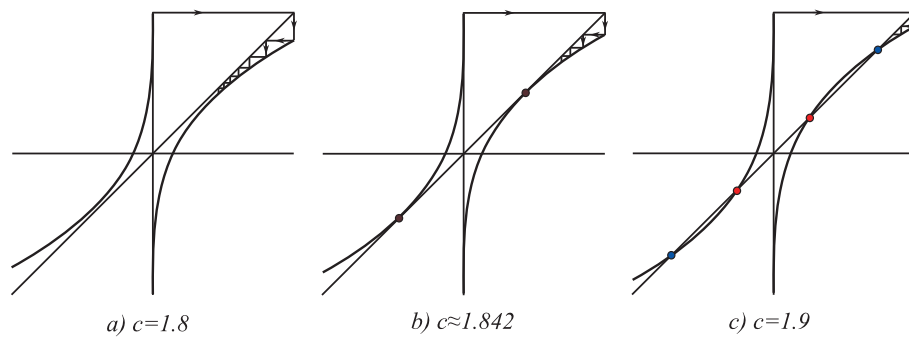


Fig. 8 Saddle-node bifurcation for $\varepsilon = 0.7$

In the region LA_1 , the map $T_{c,\varepsilon}$ is transitive, i.e., there is a dense orbit in I , and hence the attractor coincides with the whole I . One of the connected boundaries of the region LA_1 is the bifurcation curve, which corresponds

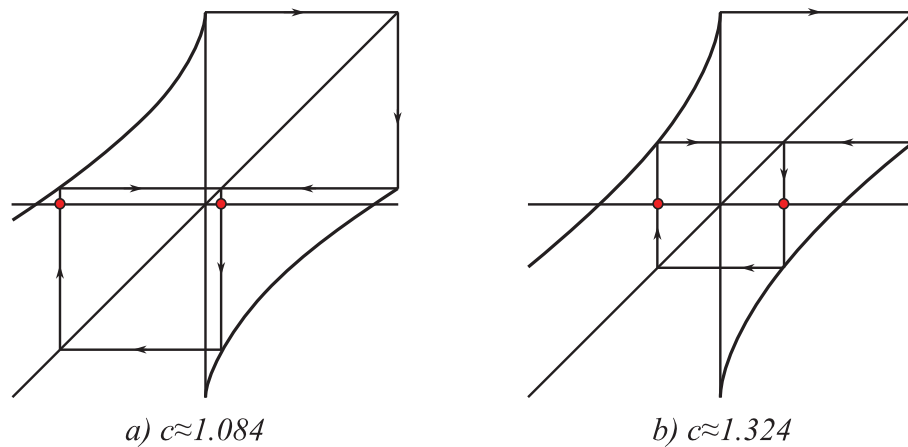


Fig. 9 Trajectory of the discontinuity point at the boundary of the LA_2 region for $\varepsilon = 0.4$.

to the case when the discontinuity point is eventually periodic (pre-periodic) to the period-2 orbit. Its equation is

$$(c-1)^{1-\varepsilon} = \frac{2-c}{c}. \quad (7)$$

Consider in more details, what happens when passing this curve. While passing from the region LA_1 to the region LA_2 , the interval $[-p, p]$, where the points $\{-p, p\}$ form the single period-2 orbit, becomes invariant under $T_{c,\varepsilon}^2$, and the restriction $T_{c,\varepsilon}^2|_{[-p,p]}$ becomes now (after scaling) a Lorenz map with the (same) discontinuity point $x = 0$. The map $T_{c,\varepsilon}^2$ is no longer transitive, and the attractor comprises now of three subintervals (connected components)

$$A = [-1, -a) \cup [-a, a] \cup (a, 1], \text{ where } a = T_{c,\varepsilon}^2(0-).$$

Note that the periodic orbit $\{-p, p\}$ ceases to belong the attractor. The corresponding trajectory in the initial flow is the saddle cycle whose stable manifolds do not intersect unstable manifolds of the attractor.

The maximal wandering intervals whose boundary contains this unstable orbit is usually called the trivial lacunae and similar definition is used for initial flow. Fig. 10 shows schematically the appearance of the trivial lacuna and the corresponding reconstructing of the attractor.

By passing from LA_2 to LA_3 , a similar bifurcation for the restriction $T_{c,\varepsilon}^2$ on appropriate interval takes place. Here, another trivial lacuna appear which corresponds to the period-4 orbit, and so on: this scenario (renormalization) appears infinitely many times. Thus, in LA_i the nonwandering set except for the attractor, contains trivial

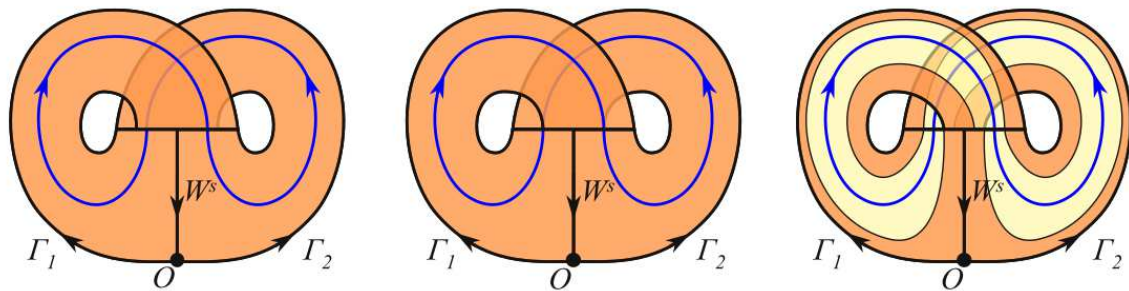


Fig. 10 Sketch of creation of the trivial lacuna

lacunae. There are countably many such regions, and they accumulate at $(0,0)$. The boundary between L_{i-1} and L_i (see red lines in fig. 4) is the bifurcation curve which corresponds to the moment when the discontinuity point becomes eventually periodic to unstable 2^i -periodic orbit. In other words, unstable separatrices of the equilibrium O are heteroclinic to the same many-round saddle cycle.

Note that the set of points corresponding to the moments when the discontinuity point is eventually periodic to the period-2 orbit, is the union of two curves (see two thick red lines in fig. 4). It is not only the boundary between the regions LA_1 and LA_2 , but also the boundary corresponding to the presence of the attractor. Through the point of intersection of these curves, the curve PF passes as well; this corresponds to the moment when a single period-2 orbit exists, and its multiplier equals 1. In this bifurcation moment the map T is transitive, and the attractor coincides with the whole I .

3 Non-monotonicity of the topological entropy

First recall the main concepts and some results of the kneading theory. The kneading theory was introduced in [12] for continuous piecewise monotone maps of the interval. In [13], the kneading theory was developed for (discontinuous) Lorenz maps and in [14] for unimodal maps along with their Lorenz models.

Let T be a Lorenz map and consider a point $x \in I$, which is not a preimage of the discontinuity point. Then the kneading sequence of x is the symbolic sequence of symbols $\{+1, -1\}$ define by

$$\omega(x) = \omega_0 \omega_1 \omega_2 \dots, \text{ where } \omega_i = \text{sgn}(T^i(x)). \quad (8)$$

Let us supply the set of one-sided sequences of symbols $\{+1, -1\}$ with the lexicographical order and the product topology (it is consistent with the distance $|\omega - \tilde{\omega}| = \sum_{i=0}^{\infty} \frac{|\omega_i - \tilde{\omega}_i|}{2^i}$). Further, one can define the kneading sequences for preimages of the discontinuity points: namely, to each preimage one associates two symbolic sequences

$$\omega^+(x) = \lim_{y \rightarrow x+0} \omega(y), \quad \omega^-(x) = \lim_{y \rightarrow x-0} \omega(y)$$

The most important are the kneading sequences of the discontinuity point $x = 0$

$$K_T^+ = \lim_{y \rightarrow 0+} \omega(y), \quad K_T^- = \lim_{y \rightarrow 0-} \omega(y)$$

Note that in the symmetric case (like for symmetric Lorenz map in the geometric model of Lorenz attractor) one has $K_T^+ = -K_T^-$.

Based on the results by M. Misiurewicz, (see, e.g. [15]), the topological entropy for a piecewise monotone map f can be calculated as the limit

$$h_{\text{top}}(f) = \lim_{k \rightarrow \infty} \frac{\log l_k}{k}, \quad (9)$$

where l_k is the number of monotonicity intervals of f^k . As was shown in [12, 13], there is an important relation between kneading invariants and the topological entropy. Namely, let us associate each symbolic sequence ω with the formal power series with the same coefficients (the generating function)

$$\omega(t) := \sum_{n=0}^{\infty} \omega_n \cdot t^n.$$

The following relation holds.

Theorem 2. *For a Lorenz map T (not necessarily symmetric) with positive topological entropy ($h_{\text{top}}(T) > 0$), the value $e^{-h_{\text{top}}(T)}$ is the minimal positive root of the function*

$$D(t) := K_T^+(t) - K_T^-(t).$$

In fact, the problem on monotonicity of topological entropy for symmetric Lorenz maps is equivalent to the problem on monotonicity of the kneading invariant K_T^+ (with respect to the lexicographical order).

Along with monotonicity of the topological entropy for the family of maps $T_{c,\varepsilon}$ we discuss here the problem of continuity of entropy as the function of the parameters. The next result is a generalization of the theorem from [13], it provides a criterion for continuity/discontinuity of the topological entropy of Lorenz maps with respect to C^0 -topology.

Theorem 3. (Malkin, Safonov, [16]) *The topological entropy may have a jump at the Lorenz map T in the space of Lorenz maps (not necessarily, symmetric) equipped with the C^0 -topology if and only if the following two conditions hold:*

1. *there is a natural number $p > 1$ such that $T^{p-1}(1) = T^{p-1}(-1) = 0$ and $T^i(1) \neq 0$, $T^i(-1) \neq 0$ for all $0 < i < p-1$,*
2. *$h_{\text{top}}(T) = 0$.*

Moreover, under the above conditions, the maximal possible jump of the topological entropy at T equals

$$\limsup_{f \rightarrow T} h_{\text{top}}(f) = \frac{1}{p} \log 2.$$

Note that for our family $T_{c,\varepsilon}$ with $c > 1$, the topological entropy is positive (it can be shown analytically; the numerical calculation see in the graph of entropy in fig. 11). Thus, it follows from the above theorem that in the whole rectangle with $c > 1$ (in fig. 4), the topological entropy changes continuously.

If $0 < c \leq 1$, then the topological entropy equals 0, and the kneading invariant is of the form

$$K_T^+ = + - + - + - \dots := (+-)^{\infty}.$$

In the green region (in fig. 4) near the axis $c = 1$, the entropy equals $\frac{\log 2}{2}$, and the kneading invariant is $K_T^+ = + - (-+)^{\infty}$. So the topological entropy has jumps as the parameter c varies at the points $(1, \varepsilon)$ for $0 < \varepsilon < 1$. In these cases the jumps due to theorem 3 has maximal possible value. In the rest of the yellow region, the kneading does not change and it equals $K_T^+ = +(-)^{\infty}$. For these maps the topological entropy coincides with that of the Bernoulli shift on two symbols, i.e., it equals $\log 2$.

For the two red thick lines in fig. 4 (given by formula 7) the kneading invariant is the same as in the yellow region below, i.e., $K_T^+ = + - (-+)^{\infty}$. Thus, if one fixes ε and considers the one-parameter family $T_c = T_{c,\varepsilon}$, then there is an entire interval of ε (approximately $\varepsilon \in [0, 0.76]$) at which the topological entropy changes non-monotonically. Numerical results suggest the conjecture that in this case the topological entropy has a single

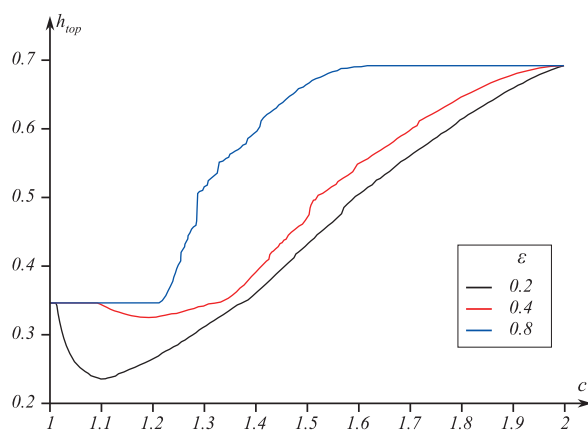


Fig. 11 The graph of topological entropy with respect to parameter c

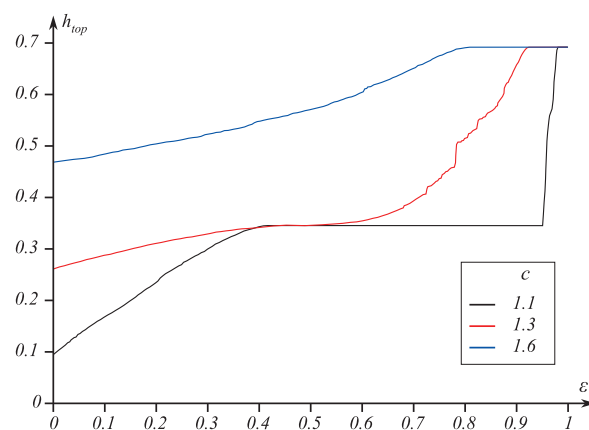


Fig. 12 The graph of topological entropy with respect to parameter ε

minimum. The graphs for several ε are shown in fig. 11. This conjecture is also consistent with the kneading chart (see fig. 5), because every vertical line $\varepsilon = \text{const}$ intersects the line of constant kneading no more than twice. Notice that at this minimum points, the line of constant kneading is tangent to the line $\varepsilon = \text{const}$.

There are numerical results (and also analytical arguments) that the region in the (c, ε) -plane, where the topological entropy $h_{top}(T_{c,\varepsilon})$ depends monotonically on c , contains the points satisfying inequalities (see fig. 5)

$$c > 1, 0 < \varepsilon < 1, c(1 - \varepsilon) > 1. \quad (10)$$

At this region the map $T_{c,\varepsilon}$ is expanding. Indeed, $\|DT_{c,\varepsilon}(x)\|_{C^0(I)} = DT_{c,\varepsilon}(1) = c(1 - \varepsilon) > 1$ because $DT_{c,\varepsilon}(x)$ has minimum at $x = \pm 1$.

Now we want to remark that even without the expanding condition above the map still can possess chaotic attractor. In particular, the next result shows that there are no stable periodic points not only in the region (10) but also in wider region, namely, above the curve PF and satisfying $DT^2(1) > 1$ (see figures 4 and 13).

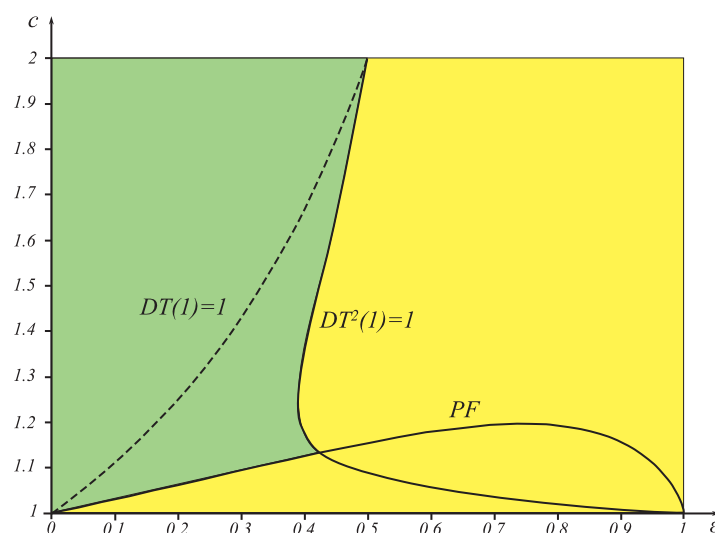


Fig. 13 Illustration to theorem 4: above the dotted line one has the expanding condition, and in the whole green region there are no stable periodic orbits. PF curve indicates the pitchfork bifurcation.

Theorem 4. For points (c, ε) in the parameters space $(1 < c < 2, 0 < \varepsilon < 1)$ lying above the curve PF

$$c(1 - \varepsilon) \cdot \left(\frac{1 - \varepsilon}{2 - \varepsilon} \right)^{-\varepsilon} > 1$$

and satisfying the condition $DT^2(1) > 1$, i.e., satisfying

$$c(1 - \varepsilon) > (c - 1)^{\varepsilon/2},$$

the map $T_{c,\varepsilon}$ has no stable periodic points.

Proof. In the proof we omit for simplicity the indexes c, ε for the map $T = T_{c,\varepsilon}$. Consider the second iteration $T^2(x)$ and find point $x \in I$, for which the derivative $DT^2(x)$ takes the minimum value. For positive $x > 0$, we have

$$\begin{aligned} \log DT^2(x) &= \log DT(T(x)) + \log DT(x) = 2 \log c(1 - \varepsilon) - \varepsilon \cdot (\log |T(x)| + \log x), \\ \frac{d}{dx} \log DT^2(x) &= -\varepsilon \cdot \left(\frac{\operatorname{sgn}(T(x)) \cdot DT(x)}{|T(x)|} + \frac{1}{x} \right) = -\varepsilon \cdot \left(\frac{DT(x)}{T(x)} + \frac{1}{x} \right). \end{aligned} \quad (11)$$

Let a be the positive preimage of 0. Then $T(x) > 0$ for $x > a$ and the expression (11) takes positive value for $x > a$. Hence,

$$\min_{x \in (a, 1]} DT^2(x) = DT^2(1) > 1 \text{ if } c(1 - \varepsilon) > (c - 1)^{\varepsilon/2}$$

For $x \in (0, a)$ the point x of minimum $\log DT^2$ satisfies the equation

$$DT(x) \cdot x = -T(x),$$

which has the unique solution

$$x^* = \left(\frac{1}{c(2 - \varepsilon)} \right)^{1/1-\varepsilon} \text{ with } T(x^*) = -\frac{1 - \varepsilon}{2 - \varepsilon}$$

From the uniqueness of the point x^* it follows that the map $T_{c,\varepsilon}$ can have at most one stable orbit of period two within the interval $(-a, a)$. Denote

$$c(1 - \varepsilon) \left(\frac{1 - \varepsilon}{2 - \varepsilon} \right)^{-\varepsilon} := \alpha,$$

Let us check that

$$DT^2(x^*) = \alpha^{(2-\varepsilon)/(1-\varepsilon)}.$$

Indeed,

$$\begin{aligned} DT^2(x^*) &= DT(x^*) \cdot DT(T(x^*)) = c(1 - \varepsilon)(x^*)^{-\varepsilon} \cdot c(1 - \varepsilon)|T(x^*)|^{-\varepsilon} = \\ &= c(1 - \varepsilon) \left(\frac{1}{c(2 - \varepsilon)} \right)^{-\varepsilon/1-\varepsilon} \cdot c(1 - \varepsilon) \left(\frac{1 - \varepsilon}{2 - \varepsilon} \right)^{-\varepsilon} = c^{(2-\varepsilon)/(1-\varepsilon)} \cdot (1 - \varepsilon)^{2-\varepsilon} \cdot (2 - \varepsilon)^{\varepsilon(2-\varepsilon)/(1-\varepsilon)} \end{aligned}$$

Recall that $\alpha = 1$ corresponds to the bifurcation curve PF. Thus, for the values of the parameters (c, ε) for which $\alpha > 1$ we have $DT^2(x) > 1$ for all $x \in I$. It follows from this fact that we have no stable periodic points: indeed, if, by contrary, T had a stable periodic point x_0 of period m then x_0 would be the stable periodic point of period $2m$, i.e. $T^{2m}(x_0) = (T^2)^m(x_0)$. On the other hand, $DT^{2m}(x_0) = DT^2(x_0) \cdot DT^2(x_2) \cdot \dots \cdot DT^2(x_{2m-2}) > 1$. The contradiction proves the theorem.

Acknowledgements. This work was partially supported by Laboratory of Dynamical Systems and Applications NRU HSE of the Ministry of science and higher education of the RF grant ag. No. 075-15-2019-1931; and by RFBR grant No. 18-29-10081. The work of K.S. was also partially supported by the RSF grant 19-71-10048. The authors thank Dr. Dmitry Turaev for posing the problem.

References

- [1] Afraimovich V.S., Bykov V.V., Shilnikov L.P. *Attractive nonrough limit sets of Lorenz-attractor type*. Trudy Moskovskoe Matematicheskoe Obshchestvo 44 (1982): 150-212.
- [2] Shilnikov L.P. *The bifurcation theory and quasi-hyperbolic attractors*. Uspehi Mat. Nauk 36 (1981): 240-241.
- [3] Robinson C. *Homoclinic bifurcation to a transitive attractor of Lorenz type*. Nonlinearity 2.4 (1989): 495.
- [4] Shilnikov A.L., Shilnikov L.P., Turaev D.V. *Normal forms and Lorenz attractors*. International Journal of Bifurcation and Chaos 3 (1993): 1123-1123.
- [5] Shilnikov A.L. *On bifurcations of the Lorenz attractor in the Shimizu-Morioka model*. Physica D: Nonlinear Phenomena 62.1-4 (1993): 338-346.
- [6] Xing T., Barrio R., Shilnikov A. *Symbolic quest into homoclinic chaos*. International Journal of Bifurcation and Chaos 24.08 (2014): 1440004.
- [7] Belykh V.N. *Bifurcation of separatrices of a saddle-point of the Lorenz system*. Differential equations 20.10 (1984): 1184-1191.
- [8] Capinski M.J., Turaev D., Zgliczynski P. *Computer assisted proof of the existence of the Lorenz attractor in the Shimizu-Morioka system*. Nonlinearity 31.12 (2018): 5410.
- [9] Douady A. *Topological entropy of unimodal maps: monotonicity for quadratic polynomials*.
- [10] Tsujii M. *A simple proof for monotonicity of entropy in the quadratic family*. Ergodic Theory Dynam. Systems, 2000, 20, p. 925-933.
- [11] Levin G., Shen W., S. van Strien. *Positive Transversality via transfer operators and holomorphic motions with applications to monotonicity for interval maps*. arXiv preprint arXiv:1902.06732 (2019).
- [12] Milnor J., Thurston W. *On iterated maps of the interval*. Dynamical systems. Springer, Berlin, Heidelberg, 1988. 465-563.
- [13] Malkin M.I. *On continuity of entropy of discontinuous mappings of the interval*. Selecta Mathematica Sovietica 8 (1989): 131-139.
- [14] Li M.-C., Malkin M. *Smooth symmetric and Lorenz models for unimodal maps*. International Journal of Bifurcation and Chaos. 13.11 (2003): 3353-3371.
- [15] Misiurewicz M., Szlenk W. *Entropy of piecewise monotone mappings*. Studia Mathematica 67.1 (1980): 45-63.
- [16] Malkin M., Safonov K. *Exact estimate on jumps of topological entropy for Lorenz- type maps*. Zhurnal SVMO 17:4 (2015) 31-36.